Sanziguben Polysaccharides Inhibit Diabetic Nephropathy Through NF-κB-Mediated Anti-Inflammation

Kang Zhou
Guangzhou University of Traditional Chinese Medicine: Guangzhou University of Chinese Medicine
jianing zhang
Guangzhou University of Chinese Medicine
Chang Liu
Guangzhou University of Traditional Chinese Medicine: Guangzhou University of Chinese Medicine
Lijuan Ou
Guangzhou University of Traditional Chinese Medicine: Guangzhou University of Chinese Medicine
Fan Wang
Guangzhou University of Traditional Chinese Medicine: Guangzhou University of Chinese Medicine
Yang Yu
Guangzhou University of Traditional Chinese Medicine: Guangzhou University of Chinese Medicine
yumei wang
Guangzhou University of Chinese Medicine
Shasha Bai (baishasha@gzucm.edu.cn)
Guangzhou University of Traditional Chinese Medicine: Guangzhou University of Chinese Medicine
https://orcid.org/0000-0002-7821-3749

Research

Keywords: Sanziguben polysaccharides, Diabetes nephropathy, inflammation

Posted Date: April 1st, 2021

DOI: https://doi.org/10.21203/rs.3.rs-362283/v1

Abstract

Background

Sanziguben polysaccharides (SZP) are large amounts of classical Chinese medicines from Sanziguben (SZGB). Moreover, SZGB is a widely applied compound prescription for diabetic nephropathy (DN) treatment.

Methods

The high-fat diet plus streptozotocin injections were used to replicate the DN models in male C57BL/6 mice. DN mice were divided into five groups: DN mice, DN mice treated with SZP(1.01 or 2.02g/kg), DN mice treated with SZGB decoction(4.7g/kg), and DN mice treated with metformin (300 mg/kg). HG and LPS plus TNFα stimulated human tubule epithelial (HK-2) cells to establish an in vitro model and treated with SZP (100 or 200 μg/mL).

Results

SZP was found to comprise sugar, protein, and uronic acid. Furthermore, SZP alleviated the progression of inflammation in vivo and in vitro by inhibiting the expression of NF-κB.

Conclusions

NF-κB plays a critical role in the development of DN induced by STZ and HG. Furthermore, SZP can attenuate the NF-κB-mediated progression of DN, which could be explored further for developing a new novel choice for the prevention and treatment of DN.

Introduction

Diabetic nephropathy (DN) is the most common diabetic microvascular complication majorly affecting the quality of human health worldwide[1, 2]. The mechanisms of DN pathogenesis are still not fully elucidated despite significant insights into DN in recent decades[3]. Blood glucose, the parameters of renal function, and histopathology have been identified as the main clinical characteristics of DN[4]. Moreover, inflammation and immune response are likely to be closely associated with the occurrence and development of DN. Clinical and experimental studies have demonstrated that excessive inflammation can lead to immune damage in the body, causing a variety of diseases and DN[1]. A study reported that monocytes from type 2 diabetes mellitus (T2DM) patients had a proinflammatory profile with a marked capacity for the expression of inflammatory cytokines. Nuclear factor-kappa B (NF-κB) significantly

promoted the development of inflammation in kidney tissues. Several studies have shown the effects of nuclear factor NF-κB p65 expression in monocytes from patients with T2DM and DN with uremia[5].

Metformin (MET) could promote pancreatic β-cell functions and decrease hepatic glucose production and intestinal glucose absorption to protect the kidney. Multiple natural compounds with various biological activities have become a treasure trove for researchers developing new drugs. Consequently, many groups have successfully confirmed that polysaccharides could regulate oxidative stress and inflammatory factors[6–8].

Sanziguben is a compound prescription made from four kinds of Chinese herbs: *Gynostemma pentaphyllum* (Thunb.) Makino, Chinese *Rosa laevigata* Michx, *Schisandra chinensis* Fructus, and *Phyllanthus emblica* and Fructus. A previous study has demonstrated that these herbs have anti-inflammatory[9] and antidiabetic[10] effects and are widely used for DN prevention[4]. Studies have shown that SZGB contains a high content of polysaccharides. Moreover, Sanziguben polysaccharide (SZP) is a polysaccharide from SZGB.

This study used the high-fat diet (HFD) plus streptozotocin (STZ)-induced mice and high glucose (HG)-treated human tubule epithelial (HK-2) cell models to assess the anti-inflammatory effects of SZP and find its possible molecular mechanism.

Materials And Methods

Plant materials

Sanziguben (SZGB) is composed of four Chinese herbs: *G. pentaphyllum* (Thunb.) Makino, Chinese *R. laevigata* Michx, *S. chinensis* Fructus, and *P.emblica* and Fructus. The crushed herbs of Schizandrae were purchased from Daxiang Pharmaceuticals Inc. (Guangzhou, China).

Chemicals

The reference standard of glucose and uronic acid were provided by Shanghai Yuanye Biotechnology Co., Ltd. (Shanghai, China). Moreover, metformin hydrochloride tablets were purchased from Sino-American Shanghai Squibb Pharmaceuticals Ltd. (Shanghai, China). STZ was obtained from Sigma-Aldrich (Sacramento, CA, USA). All test assay kits and enzyme-linked immunosorbent assay (ELISA) kits were supplied by NanJing JianCheng Bioengineering Institute (Nanjing, China). Tumor necrosis factor-alpha (TNF-α) was obtained from PeproTech Inc. (Cranbury, NJ, USA). Lipopolysaccharides (LPS) were provided by Beijing Solarbio Science & Technology Co., Ltd. (Beijing, China). NF-κB p65 (1:2,000), phospho-NF-κB p65(Ser536; 1:2,000), and phospho-IκBα (Ser32; 1:2,000) were purchased from Cell Signaling Technology (Beverly, MA, USA). The radioimmunoprecipitation assay (RIPA) lysis buffer with protease/phosphatase inhibitor cocktail, bicinchoninic acid (BCA) protein assay, anti-β-actin antibodies (1:2,000), and horseradish peroxidase (HRP)-conjugated secondary antibodies was purchased from Beijing ComWin Biotech Co., Ltd. (Beijing, China). All other chemical reagents were of analytical grade.

Extraction

Dried SZBG herbs were pulverized and screened through a 50-mesh sieve. The powder was defatted with petroleum ether for 24 h at room temperature under reflux to remove some colored materials and oligosaccharides. The residue was extracted with distilled water at 80°C twice and 2.5 h for each time after filtration. The whole extract was filtered and concentrated in a rotary evaporator under reduced pressure at 60°C for fivefold and then centrifuged at 3,000 rpm for 15 min. Moreover, the extract was then precipitated by the addition of four volumes of 95% ethanol at 4°C overnight. Moreover, the polysaccharide was obtained by centrifugation (4,000 rpm for 10 min). The solution was reprecipitated by the addition of 95% ethanol as described above, and the resultant precipitate was successively washed with anhydrous ethanol and then dried under reduced pressure to obtain SZP.

Animals

Male C57BL/6 mice (4 weeks old) were purchased from the Experimental Animal Center of Guangzhou University of Chinese Medicine (Guangdong, China). Mice were housed in a room with a temperature of 23°C ± 1°C and 55% ± 5% relative humidity with a 12-h light/12-h dark cycle. All animal experiments were approved by the Institutional Animal Care and Use Committee of Guangzhou University of Chinese Medicine (license no: SCXK 2013-0020). All animal welfare in this study followed the guidelines for ethical review of animal welfare in the People's Republic of China.

Induction of mice and drug administration

The HFD plus STZ injections were used to replicate the diabetic models in mice[11, 12]. MET is the first-line drug for the treatment of diabetes and DN[13]. Therefore, MET is selected as a positive control drug. Moreover, the mice were randomly divided into the diabetic and sham groups 1 week after adjusting to the new environment. Mice were fed with either HFD (45% of calories from fat) or standard chow diet (10% of calories from fat) for 10 weeks. Mice in the diabetic group were fed with HFD to accelerate the development of diabetic kidney disease. The diabetic group was intraperitoneally injected with 100 mg/kg STZ dissolved in citrate buffer (pH 4.0). Consequently, mice appeared hyperglycemic with fasting blood glucose (FBG) levels of 11.1–33.3 mmol/L 3 days later. The normal control group was the group that was injected with the citrate buffer without STZ. The following groups were generated for this current study: (1) Sham:normal control mice treated with distilled water (n = 20), (2) DN:diabetic mice treated with distilled water (n = 20), (3) SZP-L:diabetic mice treated with SZP (1.01 g/kg body weight/day; n a day for 8 weeks.

= 20), (4) SZP-H:diabetic mice treated with SZP (2.02 g/kg body weight/day; n = 20), (5) SZGB:diabetic mice treated with SZGB (4.7 g/kg body weight/day; n = 20), and (6)MET: diabetic treated with metformin (300 mg/kg body weight/day; n = 20). All mice were treated once

All mice were euthanized at 8 weeks after diabetes induction, and blood samples were collected and centrifuged (3,500 rpm for 10 min) to obtain serum samples. Moreover, the kidneys were removed. The

renal cortex of the kidney was isolated immediately and stored in liquid nitrogen for pathological and molecular studies.

Cultivated HG stimulates HK-2 cells

The HK-2 cells were purchased from China Center for Type Culture Collection (Wuhan, China) and grown in Dulbecco's modified eagle's medium/nutrient mixture F-12 (DMEM-F12, 1:1; GIBCO, Life Technologies, Carlsbad, CA, USA), which contained 10% fetal bovine serum (GIBCO) and 1% antibiotic–antimycotic solution (GIBCO). Cells were cultured at 37℃ in a humidified atmosphere with 5% CO_2. According to the different experiments, different stimuli were used in this study for (1) the cells to be stimulated with normal glucose as normal control, (2) for HG treatment (a final concentration of 90 mmol/L in culture medium), and (3) SZP (a final concentration of 100 or 200 μg/mL in culture medium). Moreover, all cell experiments were repeated thrice. Cell proliferation and morphology were measured using the IncuCyte ZOOM System (Essen, BioScience Inc., Ann Arbor, MI, USA).

Cultivated LPS + TNF-α stimulates HK-2 cells

HK-2 Cells were cultured at 37℃ in a humidified atmosphere with 5% CO_2 and were subcultured at 80% confluence using 0.25% trypsin-EDTA solution. The cells were exposed to DMEM-F12 containing 30 ng/mL TNF-α and 30 μg/mL LPS for 16 h to induce an inflammatory milieu. The experiments were divided into the following groups: (1) cells grown in DMEM-F12 complete medium as normal control, (2) cells stimulated by TNF-α (30 ng/mL) and LPS (30 μg/mL) for 16 h to produce inflammatory damage as a model, and (3) 100 or 200 μg/mL SZP simultaneous treatment on the model group. All cell experiments were repeated thrice. Cell proliferation and morphology were measured using the IncuCyte ZOOM System.

Chemical components and monosaccharide composition of SZP

Carbohydrate contents were measured by the phenol-sulfuric acid colorimetric method with glucose as equivalents. Protein contents were measured by Coomassie brilliant blue reaction using bovine serum albumin as the standard. Uronic acid content was determined by the carbazole-sulfuric acid method with glucuronic acid as the standard[14].

Monosaccharide composition analysis

The SZP monosaccharide compositions were analyzed by gas chromatography (GC) using an Agilent GC-6890A-5975C system equipped with a Hypercarb column. After trifluoroacetate at 121°C for hydrolysis with 2 mol/L trifluoroacetate at 121°C detected with a flame ionization detector (240°C), the column temperature was increased from 170°C for 2 min and 240°C with 6°C/min holding for 60 min. Moreover, the conversion of hydrolysate into distilled water was used as previously described[15].

Infrared spectroscopic analysis of polysaccharides

SZP was characterized by Fourier transform infrared spectroscopy (FTIR) on a Thermo Nicolet iS 5N infrared spectrophotometer (Thermo Fisher Scientific, Waltham, MA, USA) at 25°C using KBr pellets. Samples were dried at 60°C in a vacuum drying oven for 48 h before analysis, and spectra were scanned between 4,000 and 400 cm^{-1} with a resolution of 4 cm^{-1}.

Measurement of body weight, blood glucose, and urinary protein

The bodyweight of mice was measured at 2-week intervals. Blood glucose was detected using the Roche Dynamic Blood Glucose Monitoring System (Roche Inc., Mannheim, Germany) by blood sampling from the tail vein. Mice were kept separately in metabolic cages for 24-h urinary collection. Urinary protein was evaluated using the Bradford method.

Biochemical analysis

At the end of the experiment, blood samples and cell supernatants were centrifuged at 3,000×*g* for 10 min. Blood samples were separated for the detection of total cholesterol (TC), triglycerides (TG), serum creatinine (Cr) and serum urea (BUN), malondialdehyde (MDA), and catalase (CAT). The levels of the aforementioned biochemical indicators were measured using commercially available kits (Jian Cheng Bioengineering Institute, Nanjing, China). Meanwhile, the serum levels of TNF-α, monocyte chemotactic protein-1 (MCP-1), and interleukin 6 (IL-6) were measured using ELISA kits (Jian Cheng Bioengineering Institute).

Histopathological analysis

The sections of kidney tissues were removed and immediately fixed in 4% paraformaldehyde, dehydrated through a graded alcohol series, and embedded in paraffin. Moreover, 4-μm thick sections were cut using a rotary microtome and stained with hematoxylin & eosin (H&E staining), periodic acid-Schiff (PAS), and Masson's trichrome to evaluate the pathological changes of the kidney tissue. The stained specimens inspected were placed under a light microscope (Nikon, Tokyo, Japan) and imaged (×400).

Western blot analysis of NF-κB protein expression in renal tissues or HG-treated HK-2 cells

The renal tissues or cells were homogenized in an appropriate amount of protease and phosphatase inhibitor and centrifuged at 12,000 rpm for 10 min at 4℃. The protein concentration in the supernatants was scaled by utilizing the BCA protein assay kit. An aliquot of the supernatant (30 μg protein) was then suspended in a 4× loading buffer. It was then heated at 100°C for 5 min, electrophoresed on 8% sodium dodecyl sulfate-polyacrylamide gel electrophoresis (SDS-PAGE) gels at 80 V for 40 min, and then transferred onto polyvinylidene difluoride (PVDF) membranes by utilizing a Trans-Blot semidry transfer cell (Bio-Rad, Hercules, CA, USA) at 300 mA for 60 min. Moreover, 50 μg of the protein samples in each group was separated by 8% SDS-PAGE gel electrophoresis at 80 V for 30 min and then transferred onto the PVDF membrane at 300 mA for 70 min. After transferring, the PVDF membrane was blocked with 5% skim milk under room temperature for 2 h, followed by incubation with specific primary antibodies (NF-κB

p65 was diluted at 1:1,000, and β-actin was diluted at 1:1,000) at a temperature of 4°C for 16 h. The samples were then treated with anti-NF-κB p65 and anti-β-actin antibodies (Abcam Inc., Cambridge, MA, USA) under room temperature for 2 h and incubated with secondary antibody (IRDye 800CW Goat Anti-Rabbit or IRDye 800CW Goat Anti-Mouse was purchased from LI-COR, Inc., Lincoln, NE, USA). Ultimately, the bands were analyzed and quantified with Image-Pro Plus 6.0.

Western blot analysis of NF-κB protein expression in LPS + TNF-α stimulates HK-2 cells

Total protein from cells was extracted by RIPA lysis buffer with protease/phosphatase inhibitor cocktail. The BCA protein assay was performed to determine the protein concentration according to the manufacturer's instructions. The primary antibodies were as follows: NF-κB p65 (1:2,000), phospho-NF-κB p65 (Ser536; 1:2,000), phospho-IκBα (Ser32; 1:2,000), and β-actin (1:2,000). The membrane was stained with the HRP-conjugated secondary antibodies for 1 h at room temperature after being incubated with the primary antibody at 4°C overnight. The bands were presented by reacting with a chemiluminescent HRP substrate (WBKLS0100, Millipore, Germany). The intensities of individual bands were quantified with densitometric analysis using ImageJ (National Institutes of Health, Bethesda, MD, USA), and β-actin expression was considered as the internal reference.

Statistical analysis

Data are presented as mean ± standard deviation and analyzed using the Statistical Package for the Social Science, version 20.0 (SPSS 20.0, Armonk, NY, USA). Significant differences among groups were compared using analysis of variance, with $p < 0.05$ being statistically significant.

Results

Physicochemical properties of SZP

The yields of the polysaccharides extracted from defatted SZBG medicines through the hot-water extraction method and subjected to the physiochemical analyses weighed 6.22%. Conversely, SZP was a dark brown powder. The composition of SZP is summarized in Table 1. The sugar and protein contents of SZP were 54.97% and 44.17%, respectively.

Table 1 . Physicochemical properties of SZGB. Data are presented as the mean ± SD, n= 3.

Sample	Total sugar (%)	Uronic acid (%)	Protein (%)
SZP	41.6±1.49	12.4±3.8	44.17±1.1

Monosaccharide composition analysis

The monosaccharide composition of SZP was identified by comparing the relative retention time with their respective standard as well as by comparing their mass fragmentation patterns. The monosaccharide compositions of SZP are shown in Table 2. Gas chromatography–mass spectrometry analysis revealed that SZP contains mainly fucose (0.38%), arabinose (13.23%), galactose (9.75%), glucose (60.88%), xylose (1.34%), mannose (6.82%), galacturonic acid (5.54%), and glucuronic acid (2.06%).

Table 2 . Monosaccharide composition analysis of SZP

Sample	Monosaccharide composition (molar ration %)							
	Fuc	Ara	Gal	Glc	Xyl	Man	Gal-AC	Glc-AC
SZP	0.38	13.23	9.75	60.88	1.34	6.82	5.54	2.06

FTIR analysis

FTIR spectroscopy identified different functional groups, especially O–H, N–H, and C=O. The FTIR spectra of SZP are shown in Fig. 1. The strong and broad absorption peak at 3,327 cm^{-1} is attributed to the O–H stretching vibration. A weak absorbance band at around 2,938 and 2,805 cm^{-1} is a characteristic of polysaccharides, which is due to the C–H stretching and bending vibrations[16]. The strong absorption peak at 1,713 and 1,630 cm^{-1} indicates the C=O stretching vibration and the carboxyl group. The peak at 1,419 cm^{-1} results from the variable angle vibration of the N–H group, which indicated the existence of proteins. The peaks at 1,038 and 1,120 cm^{-1} belong to the C–O stretching vibration of the pyran ring. The band at 778 cm^{-1} indicated the pyran configurations of polysaccharides[16, 17].

SZP ameliorates symptoms of STZ-induced DN in mice

The HFD plus STZ-induced DN model was used in the study to evaluate the effect of SZP. The body weight and blood glucose were observed and recorded during the experiment. The food intake of the DN mice was normal, and the body weights of the sham control group mice gradually increased. However, the mice of the DN group showed weight loss, increased food intake, and reduced exercise after STZ administration. The symptoms of mice were markedly ameliorated by adding 2.02 g/kg.d dose SZP. The body weight of the SZP-H group increased compared with that of the DN group (Fig. 2A). In addition, the blood glucose of DN mice was significantly higher than that of the sham control. Furthermore, the treatment with SZP did not reverse the levels of blood glucose in these mice as shown in Fig. 2B. SZP markedly decreased the levels of blood glucose when compared with the DN group. HFD plus STZ treatment results in serious DN and leads to various blood lipid abnormalities. The obvious characteristics include the significantly higher levels of TC and TG. Moreover, the contents of TC and TG in serum were analyzed at the end of the experiment. The levels of TC and TG in the DN group were

significantly higher than those in the sham control group, and the SZP supplement reduced TC and TG (Fig. 2C, D).

Effects of SZP on the parameters of renal function in STZ-induced mice

This study tested the levels of 24-h urinary protein, serum BUN, and Cr. Compared with the sham control group, the 24-h urinary protein, serum BUN, and Cr increased in the DN group. However, they were decreased in the SZP group when compared to the DN group (Fig. 3A,B,C).

Effect of SZP on histopathological kidney changes

Histopathological changes reflect the extent of destruction and inflammation, which are obvious characteristics of DN. The hallmark includes glomerular and tubule–interstitial alterations in the kidney tissues. In this experiment, the kidney tissues were taken for H&E, PAS, and Masson's trichrome inspection. Compared with the sham group, the kidney tissues from DN group mice were severely damaged in the mucosal mesangial expansion and tubular necrosis. SZP can decrease mesangial expansion, glomerular fibrosis, hyalinosis, and interstitial inflammatory changes (Fig. 3D).

SZP suppressed the expressions of inflammatory cytokines in DN tissues

Overexpression of inflammatory cytokines, for example, TNF-α, IL-6, and MCP-1 mediators, plays a crucial role by inhibiting systemic lymphoid function and activated macrophages in DN pathogenesis. The data in this study showed that the levels of inflammatory cytokines in the sham group were extremely low, and STZ treatment was significantly increased in the kidney tissues. Moreover, adding SZP reduced the levels of inflammatory cytokines (TNF-α, IL-6, and MCP-1; Fig. 4A,B,C).

SZP downregulated the expressions of inflammatory cytokines in HG-treated HK-2 cells

Cell viability and expressions of TNF-α, IL-6, and MCP-1 were analyzed in HG-stimulated HK-2 cells to further study the inhibitory effect of SZP on the production of inflammatory cytokines. SZP does not have cytotoxic effects in HK-2 cells as shown in Fig. 5A. These results indicate that SZP could effectively reduce the levels of TNF-α, IL-6, and MCP-1 in HG-treated HK-2 cells. Compared with HG-stimulated HK-2 cells, the extremely low levels of TNF-α, IL-6, and MCP-1 were markedly prevented by a 48-h administration of SZP, especially at a dose of 200 μg/mL (Fig. 5B–D).

SZP inhibited NF-κB activation

NF-κB is involved in the pathogenesis of various diseases (e.g., inflammatory response, carcinogenesis, and apoptosis). NF-κB is an important transcriptional regulator that mediates inflammatory responses. The translocation of NF-κB p65 was analyzed in STZ-induced mice and HG-stimulated HK-2 cells to determine whether SZP inhibits inflammatory cytokine expressions by inhibiting NF-κB activation. Western blotting showed that the NF-κB p65 expression was significantly increased after STZ and HG stimulation. Adding SZP decreased the NF-κB p65 proteins (Figs. 4D and **5**E).

Effect of SZP on NF-κB pathway in LPS + TNF-α stimulates HK-2 cells

The expression levels of NF-κB and IκB proteins were detected by western blotting to investigate the role of the NF-κB pathway in SZP-treated HK-2 cells. The treatment of TNF-α and LPS upregulated NF-κB p65 and IκB proteins in HK-2 cells, whereas SZP decreased the expression of the corresponding proteins (Fig. 6). These results also suggested that SZP possessed a protective effect on the LPS + TNF-α pathway that stimulates HK-2 cells by inhibiting NF-κB.

Discussion

Growing evidence that the inflammatory processes are critical contributors to DN[18] exists. The current study observed a marked increase in inflammation levels. They were similarly impacted in both STZ-induced mice and HG-treated HK-2 cells. The upregulation of TNF-α, IL-6, and MCP-1 in kidney tissues further supports a pathogenic role in DN progression[19]. In support of these results, this study used in vitro and in vivo models and found that SZP attenuated palmitate-induced kidney damage and downregulation of inflammatory cytokines.

SZP was obtained using the hot-water extraction and alcohol precipitation method, and the physicochemical properties and activities were analyzed. SZP exhibited an obvious anti-inflammatory effect in vivo and in vitro. These results could be due to the monosaccharide composition. Previous studies have demonstrated that glucans and mannans could reduce immunological activity[20, 21]. Table 2 shows that the contents of glucose and mannose were high. According to reports, the composition of monosaccharides could be an essential factor in immunological activities[15].

DN was characterized by albuminuria, hyperglycemia, and renal injury. Moreover, inflammation is the pathogenesis of DN[5]. HFD plus STZ-induced mice could develop hyperglycemia, kidney injury, and an immune response throughout the study period. Therefore, this study proposed that the accumulation of albumin and blood glucose leads to kidney injury and inflammation. A close correlation between inflammatory cytokine overload and DN is supported by the findings that DN animal models and patients had a marked capacity for the expression of inflammatory cytokines. Therefore, this study believes that inflammation may play an important role in kidney injury.

Normally, NF-κB is a transcription factor. It could promote transcription of genes encoding proinflammatory cytokines and implicate in the pathogenesis of inflammation-related DN[22, 23]. Moreover, NF-κB is a critical factor in the regulation of immune and inflammatory responses by adjusting the expression of inflammatory cytokines. Therefore, the suppression of NF-κB activation is a very effective strategy to prevent inflammatory cytokine production in DN[24]. Thus, examining the possible molecular mechanism of SZP would be interesting. Moreover, the activation of NF-κB signaling was estimated. Strong NF-κB p65 was observed in kidney tissues of STZ-induced mice compared with the sham control group[25, 26]. Notably, the number of NF-κB p65 was reduced by SZP (Figs. 4D and 5E). Multiple pieces of evidence indicated that the levels of TNF-α were crucial for the activation of NF-κB[27]. Consequently,

investigators proposed that TNF-α may promote NF-κB transcription. Therefore, it is hypothesized that TNF-α may be a mediator for SZP to inhibit the NF-κB signaling pathway[28, 29]. The results showed that both TNF-α and NF-κB were increased in DN conditions (in DN mice and high-glucose-treated HK-2 cells) and reversed by SZP treatment (Figs. 4and 5). The NF-κB expression when LPS + TNF-α was stimulated in HK-2 cells was next detected to test whether NF-κB pathway activation involved in the anti-inflammatory effects of SZP is mediated by TNF-α. As expected, the inhibitory effect of SZP on NF-κB pathway activity was markedly by inhibiting the phosphorylation of p65 and IκBα(Fig. 6).

As an important role in DN, NF-κB may have various biological functions. For example, NF-κB has been shown to possess anti-inflammatory effects by increasing inflammation in the early stage of DN[30, 31]. In the current study, the protein expression of NF-κB and the proinflammatory mediators IL-6 and MCP-1 in the supernatant of HG-treated HK-2 cells were significantly upregulated following treatment with SZP compared with those in the sham control group. It suggests that NF-κB may act as a mediator linking tubular cell injury to interstitial IL-6 and MCP-1 in DN. The pathogenic role of NF-κB in linking DN has also been supported by recent reports showing that IL-6 and MCP-1 overexpression was associated with the activation and inhibition of the NF-κB pathway. Furthermore, the levels of NF-κB protein and the secretion of IL-6 and MCP-1 in the DN group were all higher compared with the sham control group. These results were consistent with the findings of the previous studies[32–35].

This work supports the hypothesis that SZP is a protective factor in the kidney. Moreover, SZP may be an important treatment strategy in diabetic nephropathy.

Conclusion

In conclusion, the present study preliminarily demonstrated that SZP exhibited a potent renoprotective effect. Moreover, SZP may attenuate diabetic renal lesions via the inactivation of the NF-κB signaling pathway by inhibiting TNF-α.

Abbreviations

DN:Diabetic nephropathy;T2DM: type 2 diabetes mellitus;NF-κB:Nuclear factor-kappa B; MET:Metformin;SZGB:Sanziguben;SZP:Sanziguben polysaccharides;HK-2:human tubule epithelial cells ;HFD:high-fat diet;STZ:streptozotocin; HG:high glucose;ELISA:enzyme-linked immunosorbent assay;TNF-α:Tumor necrosis factor-alpha ;LPS:Lipopolysaccharides;P-p65:phospho-NF-κB p65;P-IκBα:phospho-IκBα;RIPA:radioimmunoprecipitation assay lysis buffer;BCA:bicinchoninic acid;HRP:horseradish peroxidase;FBG:fasting blood glucose;GC:gas chromatography;FTIR:Fourier transform infrared spectroscopy ;TC:total cholesterol;TG:triglycerides;Cr:serum creatinine; BUN:serum urea; MDA:malondialdehyde; CAT:catalase; MCP-1:monocyte chemotactic protein-1;IL-6:interleukin 6;H&E staining: stained with hematoxylin & eosin;PAS:periodic acid-Schiff ;SDS-PAGE: sulfate-polyacrylamide gel electrophoresis;PVDF:polyvinylidene difluoride;

Declarations

Acknowledgements

We thank all the participants of this study

Authors' Contributions

Kang Zhou and Jianing Zhang contributed equally to this work.

Funding

This work was supported by the National Natural Science Foundation of China under grant number 81774192.

Availability of data and materials

The datasets used or analysed during the current study are available from the corresponding author on reasonable request

Ethics approval and consent to participate

All animal experiments were approved by the Institutional Animal Care and Use Committee of Guangzhou University of Chinese Medicine (license no: SCXK 2013-0020). All animal welfare in this study followed the guidelines for ethical review of animal welfare in the People's Republic of China.

Consent for publication

All authors agree with the content of the manuscript for publication.

Competing interests

The authors declare that there are no conflicts of interest.

Author details

[1] School of Pharmaceutical Sciences, Guangzhou University of Chinese Medicine.Correspondence to Shasha Bai, Email: baishasha@gzucm.edu.cn and wangym@gzucm.edu.cn Corresponding author address: Room C306, Pharmaceutical building, Guangzhou University of Chinese Medicine, No. 232 Waihuan East Road, Panyu District, Guangzhou City, Guang Dong Province, China.

References

1. Pickup JC. Inflammation and activated innate immunity in the pathogenesis of type 2 diabetes. *Diabetes Care* 2004; 27(3):813-823. doi:10.2337/diacare.27.3.813.

2. Zhang L, Zhang QM*, et al.* DNA methyltransferase 1 may be a therapy target for attenuating diabetic nephropathy and podocyte injury. *Kidney International* 2017; 92(1):140-153. doi:10.1016/j.kint.2017.01.010.
3. Zhang MH, Feng L*, et al.* The anti-inflammation effect of Moutan Cortex on advanced glycation end products-induced rat mesangial cells dysfunction and High-glucose–fat diet and streptozotocin-induced diabetic nephropathy rats. *Journal of Ethnopharmacology* 2014; 151(1):591-600.doi: 10.1016/j.jep.2013.11.015.
4. Zhang CX, Li Q*, et al.* Attenuation of diabetic nephropathy by Sanziguben Granule inhibiting EMT through Nrf2-mediated anti-oxidative effects in streptozotocin (STZ)-induced diabetic rats. *Journal of Ethnopharmacology* 2017; 205:207-216.doi: 10.1016/j.jep.2017.05.009.
5. Yang MX, Xu J*, et al.* Anti-inflammatory effects of 1,25-dihydroxyvitamin D3 in monocytes cultured in serum from patients with type 2 diabetes mellitus and diabetic nephropathy with uremia via Toll-like receptor 4 and nuclear factor-κB p65. *Molecular Medicine reports* 2015; 12:8215-8222.doi: 10.3892/mmr.2015.4482.
6. Wang J, Hu WJ*, et al.* Antidiabetic activities of polysaccharides separated from Inonotus obliquus via the modulation of oxidative stress in mice with streptozotocin-induced diabetes. *Plos One* 2017; 12(6):e0180476.doi: 10.1371/journal.pone.0180476.
7. Zhou TT, Xu X*, et al.* A preclinical overview of metformin for the treatment of type 2 diabetes. *Biomedicine and pharmacotherapy* 2018; 106:1227-1235.doi: 10.1016/j.biopha.2018.07.085.
8. Wang J, Teng L*, et al.* Studies on the antidiabetic and antinephritic activities of *Paecilomyces* hepiali water extract in diet-streptozotocin-induced diabetic sprague dawley rats. *Journal of Diabetes Research* 2016; 2016:1-10.doi: 10.1155/2016/4368380.
9. Zhang LH, Lin YF*, et al.* Simultaneous determination of gypenoside LVI, gypenoside XLVI, 2α-OH-protopanaxadiol and their two metabolites in rat plasma by LC–MS/MS and its application to pharmacokinetic studies. *Journal of Chromatography B* 2015; 1005:9-16.doi: 10.1016/j.jchromb.2015.09.028.
10. Huyen VTT, Phan DV*, et al.* Gynostemma pentaphyllum tea improves insulin sensitivity in type 2 diabetic patients. *Journal of Nutrition and Metabolism* 2016; 2013:1-7.doi: 10.1155/2013/765383.
11. Hou BY, Zhao YR*, et al.* Puerarin mitigates diabetic hepatic steatosis and fibrosis by Inhibiting TGF-β signaling pathway activation in type 2 diabetic rats. *Oxidative Medicine and Cellular Longevity* 2018; 2018:1-13.doi: 10.1155/2018/4545321.
12. Wei XY, Tao JH*, et al.* Sanhuang Xiexin Tang Ameliorates type 2 diabetic rats via modulation of the metabolic profiles and NF-κB/PI-3K/Akt signaling pathways. *Frontiers in pharmacology* 2018; 9:955.doi: 10.3389/fphar.2018.00955.
13. Wang HR, Chen Z*, et al.* Metformin and berberine, two versatile drugs in treatment of common metabolic diseases. *Oncotarget* 2015; 9(11):10135-10146.doi: 10.18632/oncotarget.20807.
14. Jia D, Rao CG*, et al.* Purification, characterization and neuroprotective effects of a polysaccharide from *Gynostemma pentaphyllum*. *Carbohydrate Polymers* 2015; 122:93-100.doi;

10.1016/j.carbpol.2014.12.032.

15. Cui L, Wang W*, et al.* Polysaccharide from Scutellaria baicalensis Georgi ameliorates colitis via suppressing NF-kappaB signaling and NLRP3 inflammasome activation. *International Journal of Biological Macromolecules* 2019; 132:393-405.doi:10.1016/j.ijbiomac.2019.03.230.
16. Zhu Y, Li Q*, et al.* Optimization of enzyme-assisted extraction and characterization of polysaccharides from Hericium erinaceus. *Carbohydrate Polymers* 2014; 101:606-613.doi: 10.1016/j.carbpol.2013.09.099.
17. Yang LQ, Zhao T*, et al.* Carboxymethylation of polysaccharides from Auricularia auricula and their antioxidant activities in vitro. *International Journal of Biological Macromolecules* 2011; 49(5):1124-1130.doi: 10.1016/j.ijbiomac.2011.09.011.
18. Fang F, Bae EH*, et al.* Deletion of the gene for adiponectin accelerates diabetic nephropathy in theIns2+/C96Ymouse. *Diabetologia* 2015; 58(7):1668-1678.doi: 10.1007/s00125-015-3605-9.
19. Tesch GH. MCP-1/CCL2: a new diagnostic marker and therapeutic target for progressive renal injury in diabetic nephropathy. *American Journal of Physiology Renal Physiology* 2008; 294(2):697-701.doi: 10.1152/ajprenal.00016.2008.
20. Tang S, Jiang MY*, et al.* Characterization of arabinogalactans from *Larix principis*-rupprechtii and their effects on NO production by macrophages. *Carbohydrate Polymers* 2018; 200:408-415.doi: 10.1016/j.carbpol.2018.08.027.
21. Taylor PR, Gordon S*, et al.* The mannose receptor: linking homeostasis and immunity through sugar recognition. *Trends in Immunology* 2005; 26(2):104-110.doi: 10.1016/j.it.2004.12.001.
22. Lawrence T, Bebien M*, et al.* IKKalpha limits macrophage NF-kappaB activation and contributes to the resolution of inflammation. *Nature* 2005; 434(7037):1138-1143.
23. Bewtra M, Brensinger CM*, et al.* An optimized patient-reported Ulcerative colitis disease activity measure derived from the Mayo Score and the simple clinical colitis activity index. *Inflammatory Bowel Diseases* 2014; 20(6):1070-1078.doi: 10.1097/MIB.0000000000000256.
24. Li Z, Zhang DK*, et al.* NF-κB p65 antisense oligonucleotides may serve as a novel molecular approach for the treatment of patients with Ulcerative colitis. *Archives of Medical Research* 2008; 39(8):729-734.doi: 10.1016/j.arcmed.2008.08.001.
25. Ouchi N, Kihara S*, et al.* Adiponectin, an adipocyte-derived plasma protein, inhibits endothelial NF-κB signaling through a cAMP-dependent pathway. *Circulation* 2000; 102(11):1296-1301.doi: 10.1161/01.cir.102.11.1296.
26. Wiecek A, Adamczak M*, et al.* Adiponectin--an adipokine with unique metabolic properties. *Nephrology Dialysis Transplantation* 2007; 22(4):981-988.doi: 10.1093/ndt/gfl814.
27. Lentsch AB, Ward PA. The NFkappaB/IkappaB system in acute inflammation. *Archivum Immunologiae et therapiae experimentalis* 2000; 48(2):59-63.
28. Krakoff J, Funahashi T*, et al.* Inflammatory markers, adiponectin, and risk of type 2 diabetes in the Pima Indian. *Diabetes Care* 2003; 26(6):1745-1751.doi; 10.2337/diacare.26.6.1745.

29. Cheng CF, Lian WS*, et al.* Protective effects of adiponectin against renal ischemia-reperfusion injury via prostacyclin-PPARα-Heme oxygenase-1 signaling pathway. *Journal of cellular physiology* 2012; 227(1):239-249.doi: 10.1002/jcp.22726.
30. Lv J, Zhang YH*, et al.* Astragalus polysaccharides protect against dextran sulfate sodium-induced colitis by inhibiting NF-κB activation. *International Journal of Biological Macromolecules* 2017; 98:723-729. doi:10.1016/j.ijbiomac.2017.02.024.
31. Kaur R, Gulati M*, et al.* Role of synbiotics in polysaccharide assisted colon targeted microspheres of mesalamine for the treatment of ulcerative colitis. *International Journal of Biological Macromolecules* 2017; 95:438-450.doi: 10.1016/j.ijbiomac.2016.11.066.
32. Rewa V, Jong Hyeok J*, et al.* 1,25-Dihydroxyvitamin D_3 up-regulates TLR10 while down-regulating TLR2, 4, and 5 in human monocyte THP-1. *The Journal of Steroid Biochemistry and Molecular Biology* 2014; 141:1-6.doi: 10.1016/j.jsbmb.2013.12.012.
33. Devaraj S, Dasu MR*, et al.* Increased toll-like receptor (TLR) 2 and TLR4 expression in monocytes from patients with type 1 diabetes: further evidence of a proinflammatory state. *The Journal of Clinical Endocrinology and Metabolism* 2008; 93(2):578-583.doi: 10.1210/jc.2007-2185.
34. Yang MX, Gan H*, et al.* Proinflammatory CD14+CD16+monocytes are associated with microinflammation in patients with type 2 diabetes mellitus and diabetic nephropathy uremia. *Inflammation* 2012; 35(1):388-396.doi: 10.1007/s10753-011-9374-9.
35. Sadeghi K, Barbara W*, et al.* Vitamin D3 down-regulates monocyte TLR expression and triggers hyporesponsiveness to pathogen-associated molecular patterns. *European Journal of Immunology* 2006; 36(2):361-370.doi: 10.1002/eji.200425995.

Figures

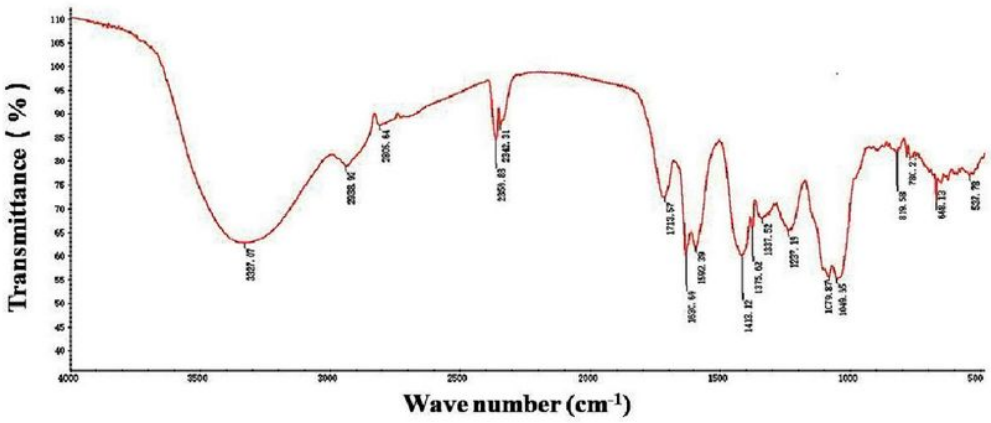

Figure 1

Fourier-transform infrared spectroscopy spectra of SZP.

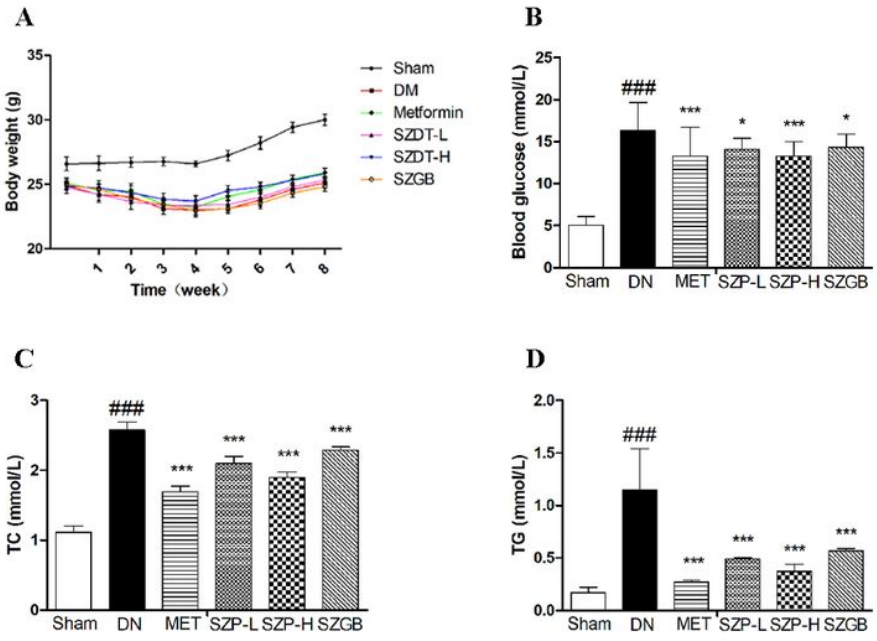

Figure 2

The effects of SZP on the parameters of body weight (A), blood glucose (B) ,blood lipids TC(C) and TG(D) in DN mice. The values presented are the means ± SD of six independent experiments and differences between mean values were assessed by ANOVA. ###P < 0.01 versus sham control group, ***P < 0.01 versus DN group and *P < 0.05 versus DN group. TC, Total cholesterol; TG, triglycerides.

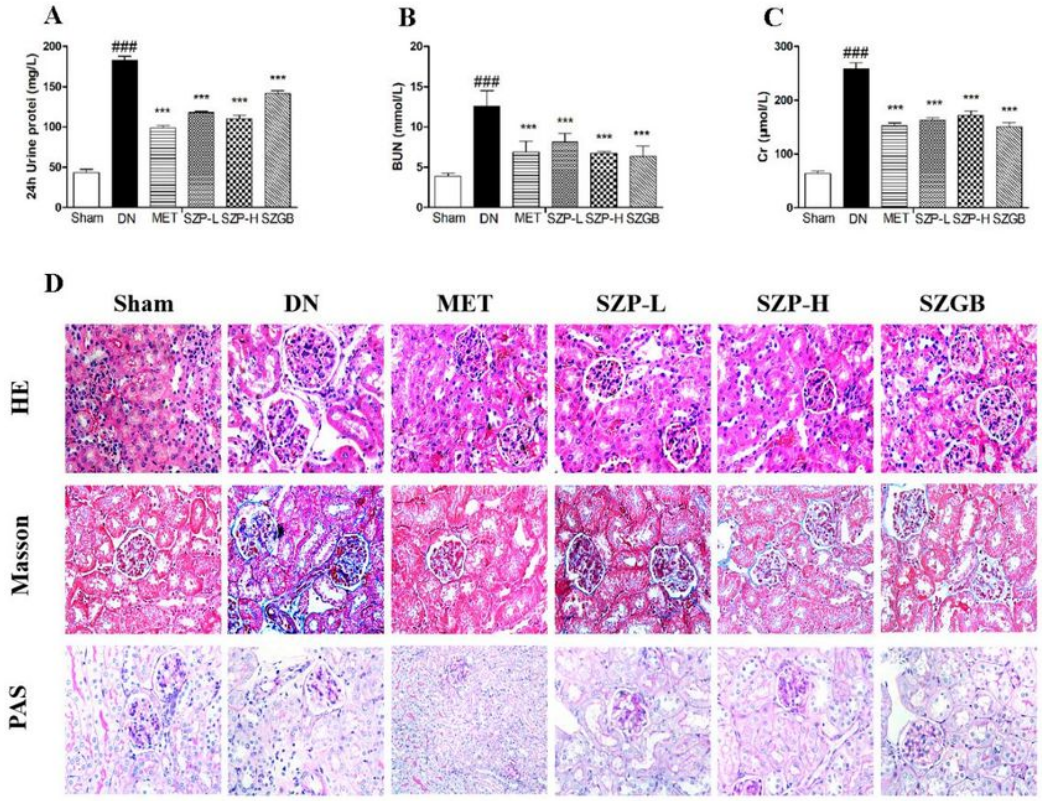

Figure 3

The effects of SZP on the parameters of renal function and kidney tissue in DN mice. The expression level of 24-h urinary protein (A). The expression level of serum BUN (B). The expression level of Cr (C). The Photomicrographs (HE, magnification ×400; PAS, magnification ×400; Masson's trichrome-stained, magnification ×400) of different groups(D).The values presented are the means ± SD of six independent experiments and differences between mean values were assessed by ANOVA. ###P < 0.01 versus sham control group, ***P < 0.01 versus DN group. Cr, serum creatinine. HE, hematoxylin and eosin; PAS, periodic acid-Schiff.

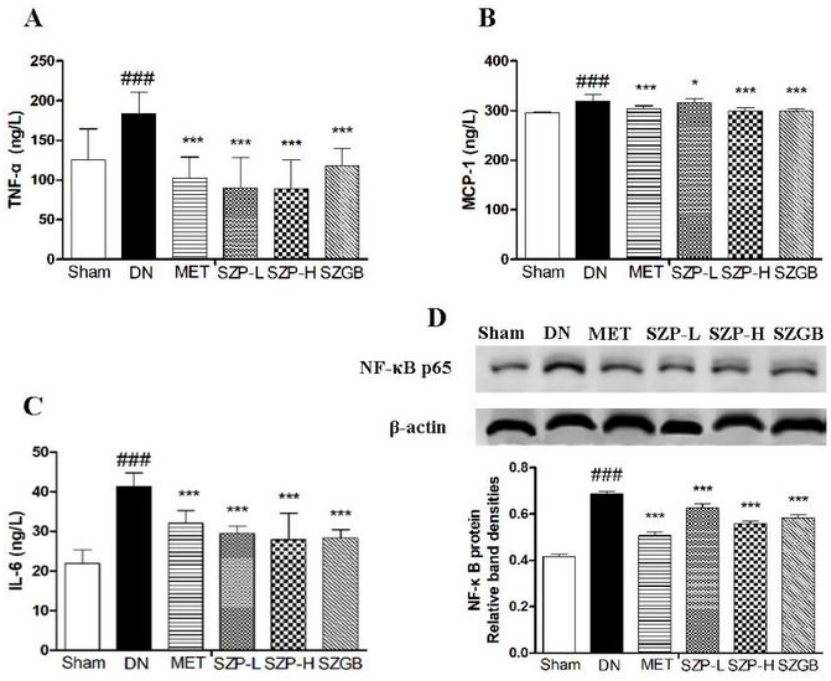

Figure 4

The effects of SZP on the secretion of inflammatory cytokines and proteins in DN mice. The expression level of TNF-α (A). The expression level of MCP-1 (B). The expression level of IL-6 (C). The values presented are the means ± SD of six independent experiments and differences between mean values were assessed by ANOVA. NF-κB protein expressions in DN mice after SZP treatment (D). The values presented are the means ± SD of three independent experiments and differences between mean values were assessed by ANOVA. ###P < 0.01 versus sham control group, ***P < 0.01 versus DN group and *P < 0.05 versus DN group. TNF-α, Tumor necrosis factor-α; MCP-1, Monocyte chemotactic protein-1; IL-6, Interleukin 6. NF-κB, Nuclear factor-kappa B.

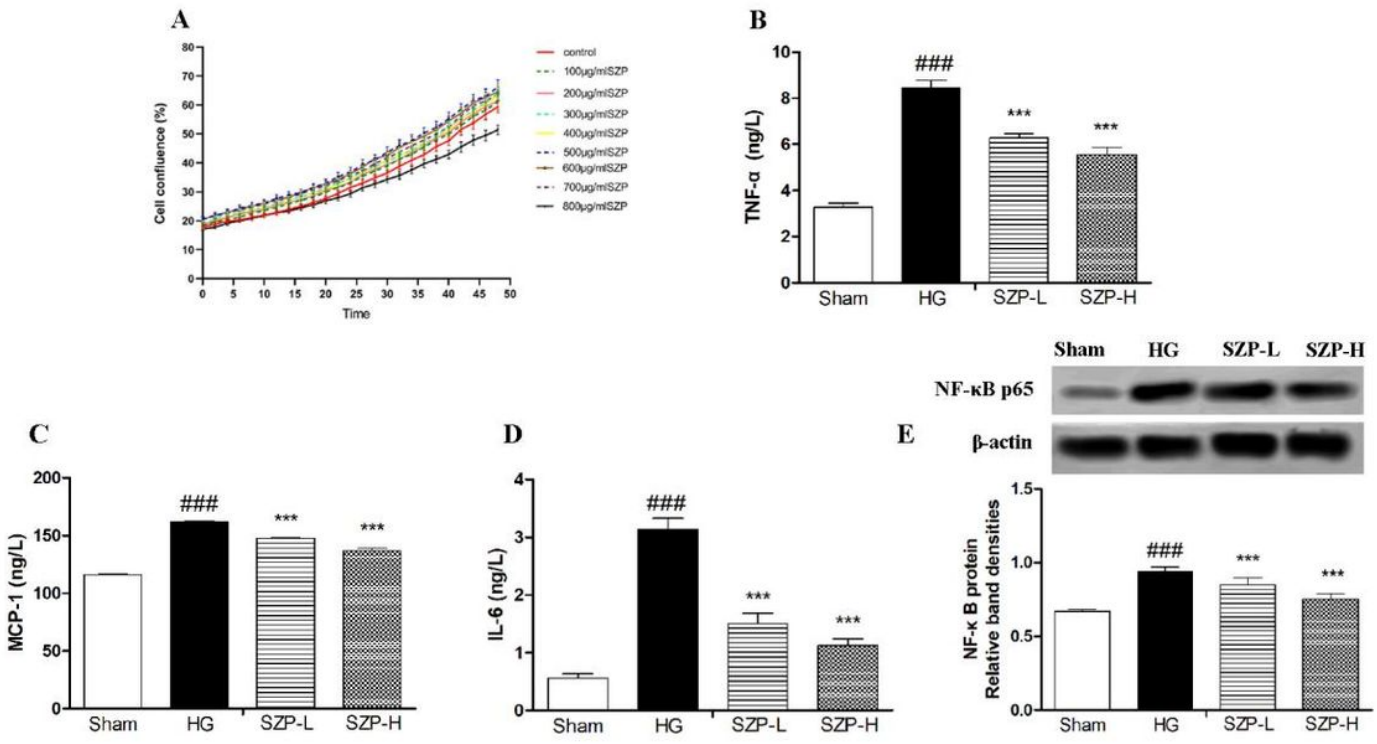

Figure 5

The effects of SZP on the secretion of inflammatory cytokines and proteins in HG-treated HK-2 cells. The cell viability of HK-2 cells after SZP treatment (A). The expression level of TNF-α (B). The expression level of MCP-1 (C). The expression level of IL-6 (D). NF-κB protein expressions in HG-stimulate HK-2 cells after SZP treatment (E). The values presented are the means ± SD of three independent experiments and differences between mean values were assessed by ANOVA. ###P < 0.001 versus sham control group, ***P < 0.001 versus HG group. HG, high-glucose; TNF-α, Tumor necrosis factor-α; MCP-1, Monocyte chemotactic protein-1; IL-6, Interleukin 6. NF-κB, Nuclear factor-kappa B.

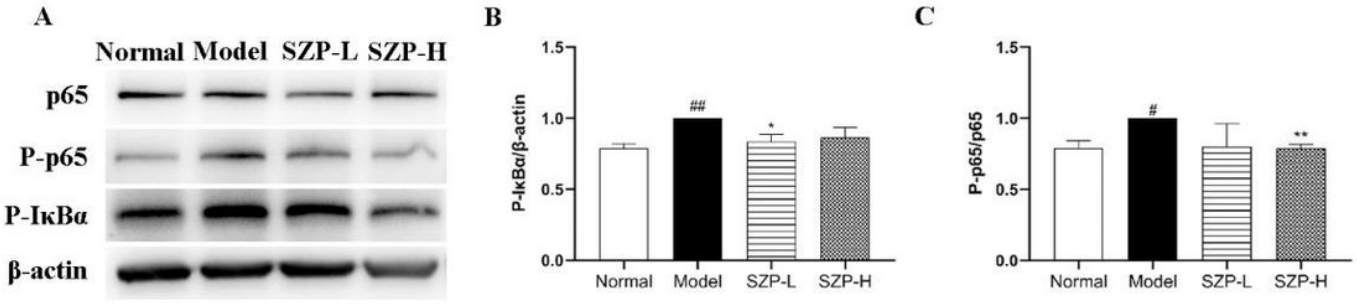

Figure 6

The effects of SZP on Western blot analysis of NF κB p65 and IκB protein expression in LPS + TNFα stimulate HK-2 cells. (A) Representative blots for NF κB p65 and IκB protein expression. (B) Bar graph showing NF κB p65 protein expression in HK-2 cells treated with LPS and TNFα. (C) Bar graph showing IκB protein expression in HK-2 cells treated with LPS and TNFα; The values presented are the means ± SD of three independent experiments and differences between mean values were assessed by ANOVA. ##P < 0.01 and #P < 0.05 versus normal control group, **P < 0.01 and *P < 0.05 versus model group. TNF-α, Tumor necrosis factor-α; NF-κB, Nuclear factor-kappa B. LPS, lipopolysaccharide.